ADVANCED DIGITAL MOTION CONTROL BASED ON MULTIRATE SAMPLING CONTROL

Hiroshi Fujimoto * **Yoichi Hori** **

* Department of Electrical Engineering, Nagaoka University of Technology, Japan, email: fujimoto@vos.nagaokaut.ac.jp
** Department of Electrical Engineering, The University of Tokyo, Japan

Abstract: In this paper, our recent studies on multirate sampling control and its application to motion control systems are reviewed. Especially, multirate two-degree-of-freedom controllers are focused on, where it is restricted that the sampling period of plant output is longer than the control period. The proposed controllers assure perfect tracking control (PTC) and perfect disturbance rejection (PDR) at M inter-sampling points. The proposed approaches are applied to the position control of servomotors, hard disk drives, and visual servo systems. The advantages are demonstrated through simulations and experiments. *Copyright © 2002 IFAC*

Keywords: multirate sampling control, motion control, tracking control, disturbance rejection, hard disk drive, visual servoing

1. INTRODUCTION

A generalized digital control system is shown in Fig. 1, where $P_c(s)$ is a continuous-time plant to be controlled, $C[z]$ is a discrete-time controller implemented in digital computer. Because the discrete-time controller has to deal with continuous-time signals, it needs to have two samplers for the reference signal $r(t)$ and the output $y(t)$, and one holder on the input $u(t)$. Therefore, there exist three time periods T_r, T_y, and T_u which represent the periods of $r(t), y(t)$, and $u(t)$, respectively. The input period T_u is generally decided by the speed of the actuator, D/A converter, or the calculation on the CPU. The output period T_y is also determined by the speed of the sensor or the A/D converter.

Actual control systems usually hold the restrictions on T_u and/or T_y. Thus, in the conventional digital control systems, these three periods are often made equal to the longer of the two periods T_u and T_y. However, multirate sampling control has been studied from the point of view both of control theories and applications [Araki, 1993]. Authors also have developed some multirate sampling controllers, and applied them to motion control systems [Fujimoto, 2000].

In this paper, our recent work on this topic is reviewed, and a part of important results is introduced. The digital control systems which have
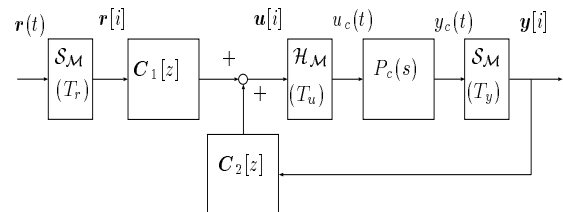

Fig. 1. Two-degree-of-freedom control system.

hardware restrictions of $T_u < T_y$ are assumed, and novel design methods of multirate two-degree-of-freedom (TDOF) controllers are proposed, which achieve perfect tracking control (PTC) and perfect disturbance rejection (PDR) at M inter-sample points in T_y. The restriction of $T_u < T_y$ may be general because D/A converters are usually faster than the A/D converters. Especially, the head-positioning systems of hard disk drives (HDDs) or the visual servo systems of robot manipulators belong to this category, because the sampling rates of measurement are relatively slow.

Recently, the modern sampled-data control theories have developed, which can optimize the inter-sample response [Chen and Francis, 1995]. In contrast, the proposed methods make simple and practical approaches to guarantee the smooth inter-sample responses by controlling all of the
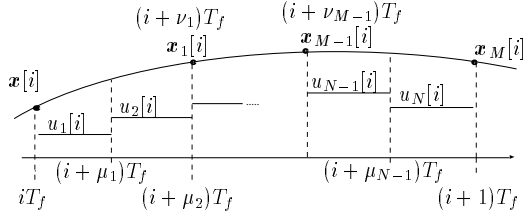
Fig. 2. Multirate sampling control.

plant states (e.g. position and velocity) at M inter-sample points.

2. DESIGN OF THE MULTIRATE TDOF CONTROLLER

In this section, new multirate TDOF controllers are proposed. For the restriction of $T_u < T_y$, the frame period T_f is defined as $T_f = T_y$ [Araki, 1993], and the dynamics of the controller is described by T_f. In the proposed multirate scheme, the plant input is changed N times during T_f and the plant state is evaluated M times in this interval as shown in Fig. 2. The positive integers N and M are referred to as input and state multiplicities, respectively. N is determined by the hardware restriction. The state multiplicity is defined as $M = N/n$, where n is the plant order.

In Fig. 2, $\mu_j(j = 0, 1, \cdots, N)$ and $\nu_k(k = 1, \cdots, M)$ are the parameters for the timing of the input changing and the state evaluation, which satisfy the conditions (1) and (2).

$$0 = \mu_0 < \mu_1 < \mu_2 < ... < \mu_N = 1 \qquad (1)$$

$$0 < \nu_1 < \nu_2 < ... < \nu_M = 1 \qquad (2)$$

If T_y is divided at same intervals, the parameters are set to $\mu_j = j/N, \nu_k = k/M$.

For simplification, the continuous-time plant is assumed to be SISO system. The proposed methods, however, can be extended to MIMO system in the same way as Fujimoto et al. [1999].

2.1 Plant Discretization by Multirate Sampling

Consider the continuous-time plant described by

$$\dot{\boldsymbol{x}}(t) = \boldsymbol{A_c}\boldsymbol{x}(t) + \boldsymbol{b_c}u(t) , \quad y(t) = \boldsymbol{c_c}\boldsymbol{x}(t). (3)$$

The discrete-time plant discretized by the multirate sampling control (Fig. 2) becomes

$$\boldsymbol{x}[i+1] = \boldsymbol{A}\boldsymbol{x}[i] + \boldsymbol{B}\boldsymbol{u}[i] , \quad y[i] = \boldsymbol{C}\boldsymbol{x}[i], (4)$$

where $\boldsymbol{x}[i] = \boldsymbol{x}(iT)$, and where matrices $\boldsymbol{A}, \boldsymbol{B}, \boldsymbol{C}$ and vector $\boldsymbol{u}$ are given by

$$\left[\begin{array}{c|c} \boldsymbol{A} & \boldsymbol{B} \\ \hline \boldsymbol{C} & \boldsymbol{O} \end{array} \right] \triangleq \left[\begin{array}{c|ccc} e^{\boldsymbol{A_c}T_f} & \boldsymbol{b}_1 & \cdots & \boldsymbol{b}_N \\ \hline \boldsymbol{c_c} & 0 & \cdots & 0 \end{array} \right], \qquad (5)$$

$$\boldsymbol{b}_j \triangleq \int_{(1-\mu_j)T_f}^{(1-\mu_{(j-1)})T_f} e^{\boldsymbol{A_c}\tau}\boldsymbol{b_c}d\tau , \quad \boldsymbol{u} \triangleq [u_1, \cdots, u_N]^T. (6)$$

The inter-sample plant state at $t = (i + \nu_k)T_f$ is represented by

$$\tilde{\boldsymbol{x}}[i] = \tilde{\boldsymbol{A}}\boldsymbol{x}[i] + \tilde{\boldsymbol{B}}\boldsymbol{u}[i], \qquad (7)$$

$$\left[\begin{array}{c|c} \tilde{\boldsymbol{A}} & \tilde{\boldsymbol{B}} \end{array} \right] \triangleq \left[\begin{array}{c|ccc} \tilde{\boldsymbol{A}}_1 & \tilde{\boldsymbol{b}}_{11} & \cdots & \tilde{\boldsymbol{b}}_{1N} \\ \vdots & \vdots & & \vdots \\ \tilde{\boldsymbol{A}}_M & \tilde{\boldsymbol{b}}_{M1} & \cdots & \tilde{\boldsymbol{b}}_{MN} \end{array} \right], \qquad (8)$$

$$\tilde{\boldsymbol{A}}_k \triangleq e^{\boldsymbol{A_c}\nu_k T_f}, \quad \tilde{\boldsymbol{x}} \triangleq [\boldsymbol{x}_1^T, \cdots, \boldsymbol{x}_M^T]^T \qquad (9)$$

$$\boldsymbol{x}_k[i] = \boldsymbol{x}[i + \nu_k] = \boldsymbol{x}((i + \nu_k)T_f), \qquad (10)$$

$$\tilde{\boldsymbol{b}}_{kj} \triangleq \begin{cases} \mu_j < \nu_k : & \int_{(\nu_k - \mu_j)T_f}^{(\nu_k - \mu_{(j-1)})T_f} e^{\boldsymbol{A_c}\tau}\boldsymbol{b_c}d\tau \\ \mu_{(j-1)} < \nu_k \le \mu_j : & \int_0^{(\nu_k - \mu_{(j-1)})T_f} e^{\boldsymbol{A_c}\tau}\boldsymbol{b_c}d\tau \\ \nu_k \le \mu_{(j-1)} : & 0 \end{cases}.$$

2.2 Design of perfect tracking controller

In the conventional digital tracking control systems, it is impossible to track the desired trajectory with zero error [Tomizuka, 1987], because the discrete-time plant discretized by the zero-order-hold usually has unstable zeros [Åström et al., 1984].

The unstable zero problem of the discrete-time plant has been resolved by zero assignment method in use of multirate control in Kabamba [1987] and Mita et al. [1990]. However, Moore et al. [1993] showed that those methods sometimes had disadvantages of large overshoot and oscillation in the inter-sample points because the control input changed back and forth very quickly. On the other hand, authors proposed perfect tracking control by introducing the multirate feedforward control, which never has this problem because all of the plant states are controlled along the smoothed desired trajectories [Fujimoto et al., 2001]. In this section, perfect tracking feedforward controller $\boldsymbol{C}_1[z]$ is designed so that the plant state ($\boldsymbol{x}$) completely tracks the desired trajectory ($\boldsymbol{x}^*$) at every sampling points $T_r(= T_y/M)$.

The control law of Fig. 1 is described by

$$\boldsymbol{u} = \boldsymbol{C}_1\boldsymbol{r} + \boldsymbol{C}_2\boldsymbol{y} \qquad (11)$$

$$= \boldsymbol{F}\hat{\boldsymbol{x}} + \boldsymbol{Q}\boldsymbol{e}_y + \boldsymbol{K}\boldsymbol{r}, \qquad (12)$$

where $\boldsymbol{K}, \boldsymbol{Q} \in \boldsymbol{RH}_\infty$ are free parameters. Therefore, Fig. 1 can be transferred to Fig. 3 [Fujimoto et al., 2001]. In the figure, $\mathcal{H}_M, \mathcal{S}$, and the thick lines represent the multirate hold, the sampler, and the multirate signals, respectively. In this paper, $\boldsymbol{K}$ becomes a constant matrix.

Because the estimation errors of the observer become zero ($\hat{\boldsymbol{x}} = \boldsymbol{x}, \boldsymbol{e}_y = 0$) for the nominal plant, from (7) and (12), this system is represented by

$$\tilde{\boldsymbol{x}}[i] = (\tilde{\boldsymbol{A}} + \tilde{\boldsymbol{B}}\boldsymbol{F})\boldsymbol{x}[i] + \tilde{\boldsymbol{B}}\boldsymbol{K}\boldsymbol{r}[i]. \qquad (13)$$
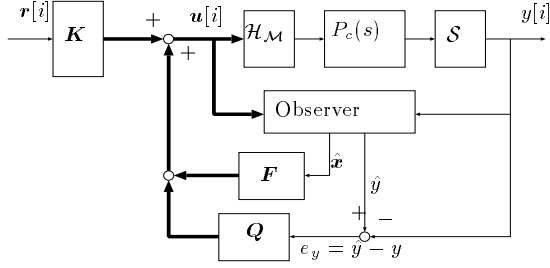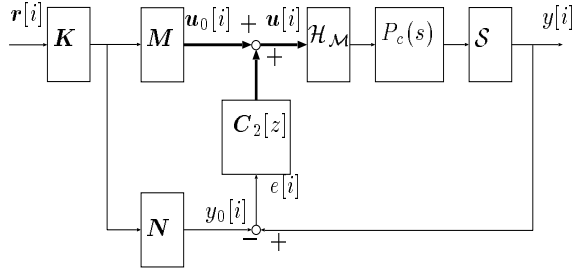
Fig. 3. Basic structure of TDOF control.

Fig. 4. Implementation of the proposed controller.

Because the non-singularity of the matrix $\tilde{B}$ is proved in Araki and Hagiwara [1986], the coefficient matrices of (13) can be arbitrary assigned by F and K. In this paper, the parameters F and K can be selected so that following equations are satisfied

$$\tilde{A} + \tilde{B}F = O \ , \quad \tilde{B}K = I. \qquad (14)$$

From (14), F and K are given by

$$F = -\tilde{B}^{-1}\tilde{A} \ , \quad K = \tilde{B}^{-1}. \qquad (15)$$

Therefore, (13) is described by $\tilde{x}[i] = r[i]$. Utilizing the previewed desired state at inter-sample points $(\tilde{x}^*[i])$, if the reference input is set to $r[i] = \tilde{x}^*[i]$, we find perfect tracking $(\tilde{x}[i] = \tilde{x}^*[i])$ can be achieved at every sampling point T_r.

Because $C_1[z]$ of (11) can be transferred to (16), $C_1[z]$ is given by

$$C_1[z] = (M - C_2 N)K, \qquad (16)$$

$$M = \left[\begin{array}{c|c} A+BF & B \\ \hline F & I \end{array} \right] = I + z^{-1}FB,$$
$$N = \left[\begin{array}{c|c} A+BF & B \\ \hline C & O \end{array} \right] = z^{-1}CB, \qquad (17)$$

as shown in Fig. 4, where M and N are the right coprime factorization of the plant $P[z] = NM^{-1}$ [Sugie and Yoshikawa, 1986, Fujimoto et al., 2001]. The initial state variable of (17) is set to be identical with the initial plant state $x[0]$. The internal stability of the proposed control system is guaranteed because $M, N \in RH_\infty$.

In the proposed scheme, $C_2[z]$ must be a robust controller which renders the sensitivity function $S[z] = (I - P[z]C_2[z])^{-1}$ sufficiently small at the frequency of the desired trajectory. The reason is that the sensitivity function $S[z]$ represents
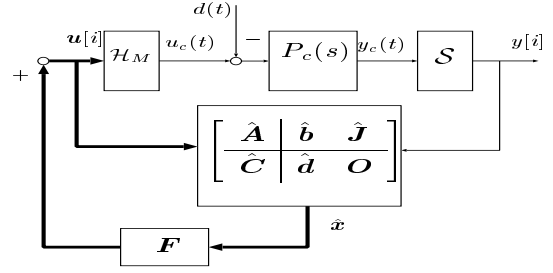

Fig. 5. Multirate control with disturbance observer.

variation of the command response $G_{yr}[z]$ under the variation of $P[z]$ [Sugie and Yoshikawa, 1986].

2.3 *Design of perfect disturbance rejection controller*

In this section, novel multirate feedback controller is proposed based on the state space design of the disturbance observer.

Consider the continuous-time plant model described by

$$\dot{x}_p(t) = A_{cp}x_p(t) + b_{cp}(u(t) - d(t)) \qquad (18)$$
$$y(t) = c_{cp}x_p(t), \qquad (19)$$

where $d(t)$ is the disturbance input. Let the disturbance model be

$$\dot{x}_d(t) = A_{cd}x_d(t) \ , \ d(t) = c_{cd}x_d(t). \qquad (20)$$

For example, the step type disturbance can be modeled by $A_{cd} = 0, c_{cd} = 1$. The continuous-time augmented system consisting of (18) and (20) is represented by

$$\dot{x}(t) = A_c x(t) + b_c u(t) \qquad (21)$$
$$y(t) = c_c x(t) \qquad (22)$$

$$A_c \triangleq \left[\begin{array}{cc} A_{cp} & -b_{cp}c_{cd} \\ O & A_{cd} \end{array} \right], b_c \triangleq \left[\begin{array}{c} b_{cp} \\ 0 \end{array} \right], x \triangleq \left[\begin{array}{c} x_p \\ x_d \end{array} \right],$$

$$c_c \triangleq [c_{cp}, 0].$$

Discretizing (21) by the multirate sampling control, the inter-sample plant state at $t = (i+\nu_k)T_f$ can be calculated from the kth row of (7) by

$$x[i + \nu_k] = \tilde{A}_k x[i] + \tilde{B}_k u[i] \qquad (23)$$

$$\tilde{A}_k = \left[\begin{array}{cc} \tilde{A}_{pk} & \tilde{A}_{pdk} \\ O & \tilde{A}_{dk} \end{array} \right], \tilde{B}_k = \left[\begin{array}{c} \tilde{B}_{pk} \\ O \end{array} \right].$$

For the plant (21) discretized by (4), the discrete-time observer on the sampling points is obtained from the Gopinath's method by

$$\hat{v}[i + 1] = \hat{A}\hat{v}[i] + \hat{b}y[i] + \hat{J}u[i] \qquad (24)$$
$$\hat{x}[i] = \hat{C}\hat{v}[i] + \hat{d}y[i]. \qquad (25)$$

As shown in Fig. 5, let the feedback control law be

$$u[i] = F_p\hat{x}_p[i] + F_d\hat{x}_d[i] = F\hat{x}[i], \qquad (26)$$

where $F \triangleq [F_p, F_d]$. Note that the F of the above equation is different from that of (12) used

in $\boldsymbol{C}_1[z]$ design. Letting $\boldsymbol{e}_v$ be the estimation errors of the observer ($\boldsymbol{e}_v = \hat{\boldsymbol{v}} - \boldsymbol{v}$), the following equation is obtained.

$$\hat{\boldsymbol{x}}[i] = \boldsymbol{x}[i] + \hat{\boldsymbol{C}}\boldsymbol{e}_v[i]. \tag{27}$$

From (23) to (27), the closed-loop system is represented by

$$\begin{bmatrix} \boldsymbol{x}_p[i+\nu_k] \\ \boldsymbol{x}_d[i+\nu_k] \\ \boldsymbol{e}_v[i+1] \end{bmatrix} = \\ \begin{bmatrix} \tilde{\boldsymbol{A}}_{pk} + \tilde{\boldsymbol{B}}_{pk}\boldsymbol{F}_p & \tilde{\boldsymbol{A}}_{pdk} + \tilde{\boldsymbol{B}}_{pk}\boldsymbol{F}_d & \tilde{\boldsymbol{B}}_{pk}\boldsymbol{F}\hat{\boldsymbol{C}} \\ \boldsymbol{O} & \tilde{\boldsymbol{A}}_{dk} & \boldsymbol{O} \\ \boldsymbol{O} & \boldsymbol{O} & \hat{\boldsymbol{A}} \end{bmatrix} \begin{bmatrix} \boldsymbol{x}_p[i] \\ \boldsymbol{x}_d[i] \\ \boldsymbol{e}_v[i] \end{bmatrix}. \tag{28}$$

Because full row rank of the matrix $\tilde{\boldsymbol{B}}_{pk}$ can be assured [Araki and Hagiwara, 1986], $\boldsymbol{F}_d$ can be selected so as to the (1,2) element of the above equation becomes zero for all $k = 1, \cdots, M$.

$$\tilde{\boldsymbol{A}}_{pdk} + \tilde{\boldsymbol{B}}_{pk}\boldsymbol{F}_d = \boldsymbol{O} \tag{29}$$

The simultaneous equation of (29) for all k becomes

$$\tilde{\boldsymbol{A}}_{pd} + \tilde{\boldsymbol{B}}_p\boldsymbol{F}_d = \boldsymbol{O}, \tag{30}$$

$$\begin{bmatrix} \tilde{\boldsymbol{A}}_{pd} & \tilde{\boldsymbol{B}}_p \end{bmatrix} \triangleq \begin{bmatrix} \tilde{\boldsymbol{A}}_{pd1} & \tilde{\boldsymbol{B}}_{p1} \\ \vdots & \vdots \\ \tilde{\boldsymbol{A}}_{pdM} & \tilde{\boldsymbol{B}}_{pM} \end{bmatrix}. \tag{31}$$

From (30), $\boldsymbol{F}_d$ is obtained by

$$\boldsymbol{F}_d = -\tilde{\boldsymbol{B}}_p^{-1}\tilde{\boldsymbol{A}}_{pd}. \tag{32}$$

On (28) and (29), the influence from disturbance $\boldsymbol{x}_d[i]$ to the inter-sample state $\boldsymbol{x}_p[i+\nu_k]$ at $t = (i+\nu_k)T_f$ can become zero. Moreover, $\boldsymbol{x}_p[i]$ and $\boldsymbol{e}_v[i]$ at the sampling point converge to zero at the rate of the eigenvalues of $\tilde{\boldsymbol{A}}_{pM} + \tilde{\boldsymbol{B}}_{pM}\boldsymbol{F}_p$ and $\hat{\boldsymbol{A}}$ (the poles of regulator and observer). Therefore, perfect disturbance rejection is achieved ($\boldsymbol{x}_p[i+\nu_k] = 0$) in the steady state. The poles of regulator and observer should be tuned by the tradeoff between the performance and stability robustness.

3. APPLICATIONS TO MOTION CONTROL

3.1 *Position control of servomotor by PTC*

In this section, perfect tracking control (PTC) proposed in section 2.2 is applied to the position tracking control system of a servomotor [Fujimoto et al., 2001]. First, the simplest example of $T_y = T_u$ is considered. The servomotor with current control is described by

$$P_c(s) = \frac{K}{Js^2}. \tag{33}$$

The discrete-time plant with zero-order-hold is obtained by

$$P[z] = \frac{T^2 K}{2J} \frac{z+1}{(z-1)^2}, \tag{34}$$
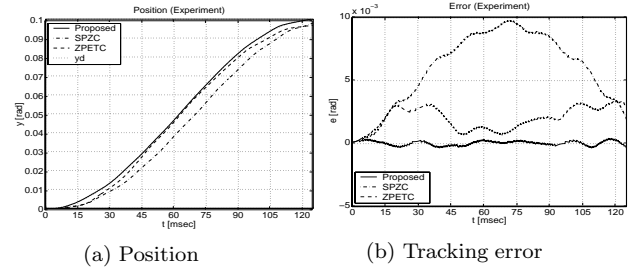

(a) Position   (b) Tracking error
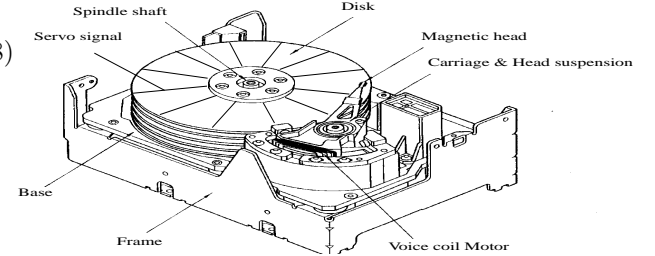
Fig. 6. Experimental results of PTC for servomotor

Fig. 7. Hard disk drive.

where T is the sampling period. Because it has an unstable zero at -1, perfect tracking control is impossible in the single-rate system. Thus, the proposed multirate feedforward control is applied.

Experimental results under the desired sinusoidal trajectories of 4 [Hz] are shown in Fig. 6. In this system, both input and output periods are $T_y = T_u = 15$[ms]. Because this plant is a 2nd-order system, the sampling period of the reference signal becomes $T_r = 30$[ms] ($N = 2$). The robust feedback controller $C_2[z]$ is previously designed by H_∞ theory.

In the following experiments, the proposed method is compared with both SPZC (Stable Pole Zero Cancelling) and ZPETC (Zero Phase Error Tracking Control) proposed by Tomizuka [1987], at the same T_y and T_u. Therefore, the reference sampling period T_r of the proposed method is twice as long as those of SPZC and ZPETC, because these methods are single-rate approaches and their sampling periods are set to $T_y = T_u = T_r = 15$[ms]. In spite of that, the results of proposed method have better tracking performance than those methods.

Fig. 6(a) and (b) show that the proposed method exhibits better performance than either SPZC or ZPETC. While the responses of SPZC and ZPETC include large tracking errors caused by the unstable zero, those of the proposed method have small tracking error. Fig. 6 also shows that the intersample responses are very smooth, because not only position but also velocity follow the desired trajectories at every sampling point T_r.

3.2 *Seeking control of hard disk drive by PTC*

In the servo systems of HDDs, the head position is detected by the discrete servo signals embedded in
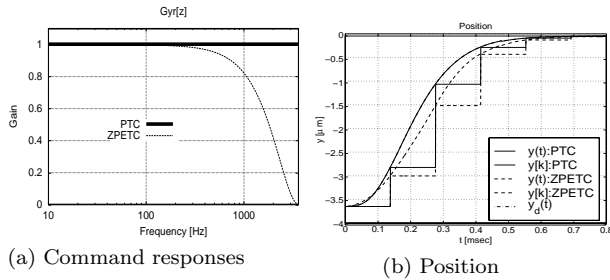
(a) Command responses

(b) Position

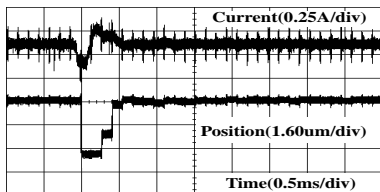Fig. 8. Simulation results of PTC for HDD

Fig. 9. Experimental results of PTC for HDD

the disks, as shown in Fig. 7. Therefore, the output sampling period T_y is decided by the number of these signals and the rotational frequency of the spindle motor. However, it is possible to set the control period T_u shorter than T_y because of the recent development of CPU. Thus, the controller can be regarded as the multirate system which has the hardware restriction of $T_u < T_y$.

In this section, the proposed PTC is applied to seeking control of 3.5-in hard disk drive [Fujimoto and Hori, 2002]. The plant is modeled by double integrator system with time delay. Thus, the proposed method has extended to systems with time delay in Fujimoto [2000]. The sampling time of this drive is $T_y = 138.54$ [μs], and the control input can be changed $N = 4$ times during this period. Because the plant is second order system ($n = 2$), perfect tracking is assured $N/n = 2$ times during sampling period.

The actual plant has the first mechanical resonance mode around 2.7 [kHz]. The Nyquist frequency is also 3.6 [kHz]. In spite of those, the target seeking-time is set to 3 sampling time (2.4 [kHz]) for one track seeking in these experiments.

The frequency responses from the desired trajectory $y_d[i]$ to the output $y[i]$ are shown in Fig. 8(a). Because the proposed method (PTC) assures perfect tracking, the command response becomes 1 in the all frequency. However, the gain of ZPETC decreases in the high frequency. The frequency of the short-span seeking is 2 [kHz] around. Therefore, the proposed method has advantages in fast seeking control.

Fig. 8(b) shows simulation results of the short-span seeking (1 [trk]), which shows that the proposed method gives better performance than ZPETC. Fig. 9 shows that the seeking time of the proposed method gets to about 3 sampling time in the experiments.

Table 1. Experimental seeking-time.

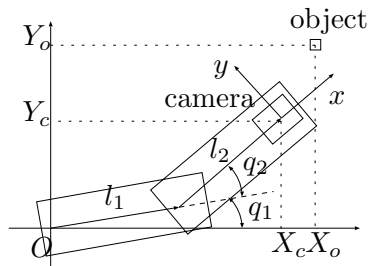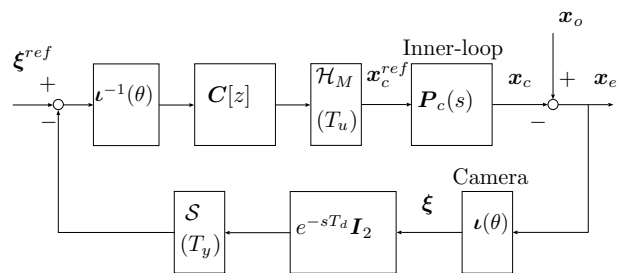|	PTC	ZPETC	Conventional
1trk	$3.17T_s$	$3.77T_s$	$4.14T_s$
6trk	$8.66T_s$	$9.57T_s$	$14.0T_s$

Fig. 10. Two-link DD robot with camera.

Fig. 11. Visual servo system.

Table 1 shows the average seeking-time which is measured in the 2000 times experiments. The seeking-time of the proposed method (PTC) is much smaller than that of ZPETC and the conventional settling control [Yamaguchi et al., 1998].

3.3 Visual servoing of robot manipulator by PDR

In this section, perfect disturbance rejection (PDR) proposed in section 2.3 is applied to the visual servo problem [Fujimoto and Hori, 2001], in which the camera mounted on the robot manipulator tracks a moving object as shown in Fig. 10. Although the sampling period of vision sensor such as a CCD camera is comparatively slow (over 33 [ms]), the control period of joint servo is fast (less than 1 [ms]). Therefore, multirate controllers have been developed and implemented in the visual servo system (e.g. Hashimoto and Kimura [1995]).

Fig. 11 shows the proposed control system. First, the work space position controller is designed to control the camera position [Murakami et al., 1995]. Letting $\boldsymbol{x}_c^{ref}(= [X_c^{ref}, Y_c^{ref}]^T)$ be the control input $\boldsymbol{u}$ of the outer vision loop, the inner-loop is regarded as analog system because the sampling period of the inner-loop is very short (1 [ms] in this experiment). The desired feature $\boldsymbol{\xi}^{ref}$ is set to zero because the camera is controlled to be positioned just below the object. The movement of the object can be modeled as the output disturbance $\boldsymbol{x}_o$. Therefore, the proposed method can achieve high tracking performance, because the periodic

(a) Feature error ξ_x

(b) Control input X_c^{ref}
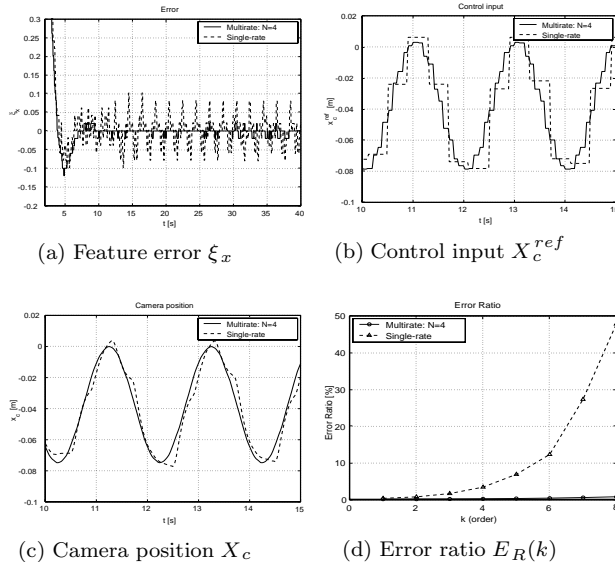

(c) Camera position X_c

(d) Error ratio $E_R(k)$

Fig. 12. Experimental results of PDR for visual servo system ($T_y = 400$ [ms], $N = 4$).

motion modeled by (35) can be rejected by the proposed PDR.

$$d(t) = a_0 + \sum_k a_k \cos k\omega_0 t + b_k \sin k\omega_0 t \quad (35)$$

Moreover, the control system of Fig. 11 is linearized and diagonalized by the inverse of the perspective transformation $\iota^{-1}(\theta)$. Thus, the controllers can be designed independently in the x and y axes. In Fig. 11, e^{-sT_d} expresses the time delay caused by image processing.

The experimental results are shown in Fig. 12. In these experiments, the image is detected at every 100 [ms]. In order to display the intersample response, the sampling period is set to $T_y = 400$ [ms] in the controller. Fig. 12(a) shows that the tracking error of the proposed multirate controller is much smaller than that of the single-rate controller in the image plane. Moreover, as shown in Fig. 12(b) and (c), the camera position is very smooth because the multirate controller generates the intersample position reference based on the disturbance model. Note that the amplitude and phase of the target movement are assumed to be unknown, and the information is estimated by the observer. Fig. 12(d) shows the calculated results of error ratio for the object velocity. While the conventional single-rate controller has large error for high speed movement, the proposed method has very small error.

4. CONCLUSION

In this paper, our recent research on multirate sampling control for motion control system was reviewed. Particularly, the digital control systems which have hardware restrictions of $T_u < T_y$ were assumed, and the multirate feedforward controller was proposed, which assured perfect tracking at M inter-sample points. Next, the multirate feedback controller was proposed, which guaranteed perfect disturbance rejection at M inter-sample points in the steady state. The proposed approaches were applied to the position control of servomotors, hard disk drives, and visual servo systems, and the advantages were demonstrated through simulations and experiments.

References

M. Araki. Recent developments in digital control theory. In *12th IFAC World Congress*, volume 9, pages 251–260, July 1993.

M. Araki and T. Hagiwara. Pole assignment by multirate-data output feedback. *Int. J. Control*, 44(6):1661–1673, 1986.

K. J. Åström, P. Hangander, and J. Sternby. Zeros of sampled system. *Automatica*, 20(1):31–38, 1984.

T. Chen and B. Francis. *Optimal Sampled-Data Control Systems*. Springer, 1995.

H. Fujimoto, A. Kawamura, and M. Tomizuka. Generalized digital redesign method for linear feedback system based on N-delay control. *IEEE/ASME Trans. Mechatronics*, 4(2):101–109, 1999.

H. Fujimoto. *General Framework of Multirate Sampling Control and Applications to Motion Control Systems*. PhD thesis, The University of Tokyo, December 2000.

H. Fujimoto and Y. Hori. Visual servoing based on intersample disturbance rejection by multirate sampling control – time delay compensation and experimental verification –. In *Conf. Decision Contr.*, pages 334–339, 2001.

H. Fujimoto and Y. Hori. High-performance servo systems based on multirate sampling control. *Control Engineering Practice*, 2002. (to be published).

H. Fujimoto, Y. Hori, and A. Kawamura. Perfect tracking control based on multirate feedforward control with generalized sampling periods. *IEEE Trans. Industrial Electronics*, 48(3):636–644, 2001.

K. Hashimoto and H. Kimura. Visual servoing with nonlinear observer. *IEEE Int. Conf. Robotics and Automation*, pages 484–489, 1995.

P. T. Kabamba. Control of linear systems using generalized sampled-data hold functions. *IEEE Trans. Automat. Contr.*, 32(9):772–783, 1987.

T. Mita, Y. Chida, Y. Kazu, and H. Numasato. Two-delay robust digital control and its applications – avoiding the problem on unstable limiting zeros. *IEEE Trans. Automat. Contr.*, 35(8):962–970, 1990.

K. L. Moore, S. P. Bhattacharyya, and M. Dahleh. Capabilities and limitations of multirate control schemes. *Automatica*, 29(4):941–951, 1993.

T. Murakami, N. Oda, Y. Miyasaka, and K.Ohnishi. A motion control strategy based on equivalent mass matrix in multidegree-of-freedom manipulator. *IEEE Trans. Industrial Electronics*, 42(2):259–265, 1995.

T. Sugie and T. Yoshikawa. General solution of robust tracking problem in two-degree-of-freedom control systems. *IEEE Trans. Automat. Contr.*, 31(6):552–554, 1986.

M. Tomizuka. Zero phase error tracking algorithm for digital control. *ASME, J. Dynam. Syst., Measur., and Contr.*, 109:65–68, March 1987.

T. Yamaguchi, H. Numasato, and H. Hirai. A mode-switching control for motion control and its application to disk drives: Design of optimal mode-switching conditions. *IEEE/ASME Trans. Mechatronics*, 3(3):202–209, 1998.